**Nanocrystals**

# Exceptionally Mild Reactive Stripping of Native Ligands from Nanocrystal Surfaces by Using Meerwein's Salt**

*Evelyn L. Rosen, Raffaella Buonsanti, Anna Llordes, April M. Sawvel, Delia J. Milliron, and Brett A. Helms**

Native coordinating ligands acquired during the chemical synthesis of colloidal nanocrystals are optimized primarily for their ability to exert control over nanocrystal size, composition, morphology, and dispersibility, and not necessarily for their final application.[1] In general, they are hydrophobic and highly insulating, and constitute a significant barrier for charge or ion transport in devices configured therefrom. Bare nanocrystal surfaces, while desirable for many applications, can be difficult to obtain reliably and without undesirable consequences. For example, removal of native ligands from nanocrystal dispersions usually results in aggregation or etching,[2] while in thin films their chemical displacement (e.g., by hydrazine or formic acid) often gives inefficient removal of surface ligands.[3] Thermal treatments inevitably leave behind an undesirable residue, require lengthy annealing times, or result in particle sintering.[4] Nevertheless, these approaches have demonstrated that near-bare nanocrystal surfaces are useful in a broad spectrum of advanced energy applications, from light-emitting diodes to field-effect transistors and photovoltaics.[5,6] Dispersions of bare nanocrystals would also be useful as nanoinks and for facilitating their transfer into polar media for biomedical applications and catalysis.[7] In pursuit of a universal reagent for producing stable dispersions or thin films of ligand-stripped nanocrystals with retention of their physical properties, we show here that this can be uniquely achieved by using Meerwein's and other trialkyl oxonium salts.[8]

[*] Dr. E. L. Rosen, Dr. R. Buonsanti, Dr. A. Llordes, Dr. A. M. Sawvel, Dr. D. J. Milliron, Dr. B. A. Helms
The Molecular Foundry, Lawrence Berkeley National Laboratory
One Cyclotron Road, Berkeley, CA 94720 (USA)
E-mail: BAHelms@lbl.gov
Homepage: http://foundry.lbl.gov/six/organic/staff-
Brett_Helms.html

Supporting information for this article is available on the WWW under http://dx.doi.org/10.1002/anie.201105996.

Recently, $NOBF_4$ was proposed as a general reagent for stripping of oleate ligands from metal oxides, metals, dielectrics, and some semiconductors.[9] While this technique is quite effective for certain nanocrystals, it is not applicable to materials with limited chemical stability, which include most metal chalcogenides and some important oxides, such as both doped and undoped ZnO,[10] presumably due to the oxidative ability and Lewis acidity of the nitrosonium cation.[11] Acids such as $HBF_4$ and $HPF_6$ have also been explored recently[12] for removal of native ligands; however, as acids etch many nanocrystals, their utility as general ligand-stripping agents has not been demonstrated. We hypothesized that these problems could be overcome by employing nonoxidizing and nonacidic reagents that would undergo targeted reactions with coordinating ligands and render them incapable of interacting with the nanocrystal surface. In related work by us and others,[13] reactive ligand exchange was possible by using trimethylsilylating agents which react with oxoanionic ligands to produce noncoordinating trimethylsilyl esters. While extremely useful for placing unique functionality at the nanocrystal surface, this approach does not yield a "bare" surface. By employing trialkyl oxonium salts instead, we proposed to exploit their superior alkylating character to rapidly and efficiently remove a broad spectrum of native ligand types while leaving the surface of the nanocrystal bare, with ligands (e.g., $BF_4^-$ or $PF_6^-$) weakly coordinating through electrostatic interactions in their place (Scheme 1). Since trialkyl oxonium salts are unreactive toward inorganic constituents such as chalcogenides, we hoped to achieve a broader substrate scope, and pave the way to more robust chemical treatments to activate nanocrystal surfaces.
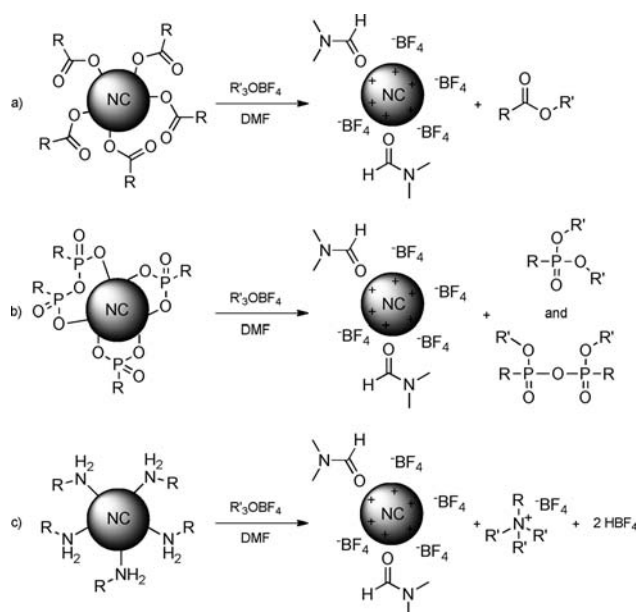
As a test case to evaluate the applicability of our approach, we investigated the utility of Meerwein's salt ($Et_3OBF_4$) for reactive ligand stripping of oleate-passivated lead selenide nanocrystals (PbSe-OA), which has been especially problematic for reasons that remain elusive.[2b,4e] Nevertheless, PbSe is an exceptionally important electronic material due to its large Bohr radius, narrow band gap, and efficient multiple-exciton generation.[14] Native ligand removal from PbSe nanocrystal thin films would not only be highly desirable for next-generation device applications, but would also provide a unique opportunity to develop a comprehensive analytical framework to evaluate the stripping process, which would help elucidate the mechanistic aspects of this and related chemistries that have not emerged from previous studies.[3a,5]

Ligand-stripping reactions on ordered films of PbSe-OA deposited on Si substrates were studied by immersion of the films in dilute solutions of $Et_3OBF_4$ in acetonitrile (MeCN)

**Scheme 1.** Reactive ligand stripping of carboxylate-, phosphonate-, and amine-passivated nanocrystals with trialkyloxonium salts.
a) NC = CdSe, CdSe/CdS, PbSe, TiO$_2$, α-Fe$_2$O$_3$, ZnO, doped NaYF$_4$, etc.
b) NC = CdSe, CdSe/ZnS, etc. c) NC = doped In$_2$O$_3$, Ag, FePt, etc.



**Figure 1.** SEM images of a) an ordered superlattice of PbSe-OA and b) a bare PbSe thin film after treatment with Et$_3$OBF$_4$ in DMF/MeCN. Scale bars are 50 nm. TEM images of c) PbSe-OA and d) PbSe-OA treated with Et$_3$OBF$_4$ in MeCN. Scale bars are 10 nm for the lower-magnification images and 2 nm for the high-resolution inset.

(50 mM). In addition, we also studied ligand stripping in the presence of two highly polar cosolvents, *N,N*-dimethylformamide (DMF) and hexamethylphosphoramide (HMPA), to determine whether these molecules would weakly coordinate through their oxygen atoms to the bare nanocrystal surfaces. Trialkyl oxonium salts are well known to react with both DMF and HMPA to yield activated species which should also serve as efficient alkylating agents.[15]

The SEM and TEM images of the initial and oleate-stripped films are shown in Figure 1. For the reaction of PbSe-OA and Et$_3$OBF$_4$ in MeCN, 1M DMF in MeCN, or 1M HMPA in MeCN (Figure 1 and Figure S2 of the Supporting Information), the stripped films exhibited visibly decreased interparticle spacing, consistent with oleate removal.[16] For comparison, treating PbSe-OA on Si with NOBF$_4$ in MeCN resulted in complete destruction of the structural integrity of the particles (Supporting Information, Figure S2). Analysis of the Et$_3$OBF$_4$-treated nanocrystal films by energy-dispersive X-ray spectroscopy (EDS) revealed drastic reduction in the carbon signal relative to PbSe-OA (Figure 2a). Notably, no fluorine was detected. For the film treated with NOBF$_4$, EDS revealed only Se and background levels of C and O (Supporting Information, Figure S3). This confirmed the oxidizing potential of NOBF$_4$ when used for PbSe, as the absence of Pb shown by EDS suggested oxidation of Se$^{2-}$ to Se$^0$ with concomitant formation of soluble [Pb(MeCN)$_n$]-(BF$_4$)$_2$.

We next sought to identify any molecules left on the stripped PbSe surface, which can be studied by FTIR spectroscopy (Figure 2b). As expected, PbSe-OA nanocrystal thin films exhibited diagnostic signals for oleate ligands around 2900 cm$^{-1}$ (symmetric and antisymmetric CH stretches) and 1450 cm$^{-1}$ (symmetric and antisymmetric
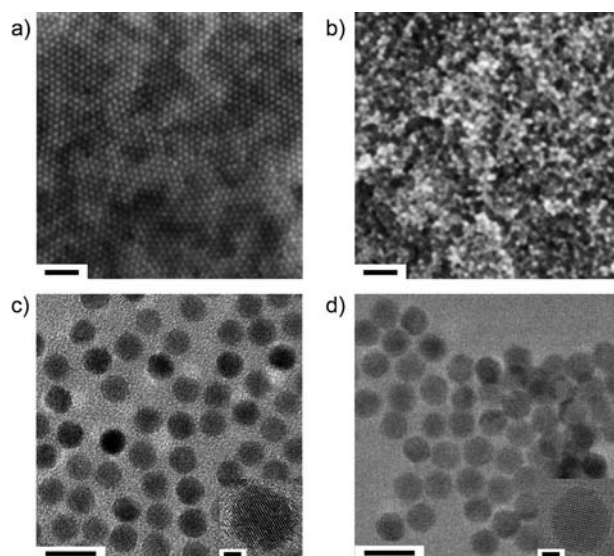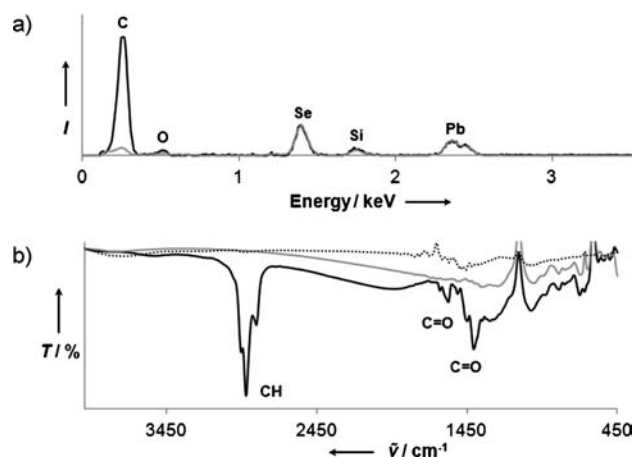


**Figure 2.** a) EDS of thin films of nanocrystalline PbSe-OA (black) and PbSe-OA treated with Et$_3$OBF$_4$ in MeCN (gray) obtained at 5 kV and scaled to Se for comparison. b) FTIR spectra for thin films of nanocrystalline PbSe-OA (black) and resulting films after Et$_3$OBF$_4$ ligand stripping in MeCN (gray) and DMF/MeCN (black dots) on double-side-polished Si substrates.

carbonyl stretches).[5b] After treatment with Et$_3$OBF$_4$ in MeCN, these signals were completely absent. Surprisingly, no stretching band attributable to BF$_4^-$ was present at 1080 cm$^{-1}$. Also, for PbSe-OA thin films treated with Meerwein-activated DMF, signals attributed to surface-adsorbed DMF were not present, as no carbonyl stretching band was observed around 1650 cm$^{-1}$.[9,17] Collectively, the absence of signals attributable to BF$_4^-$ and solvent molecules by EDS and FTIR analysis suggested that the cosolvent and counterion were not involved in passivation of stripped PbSe nanocrystal surfaces. We surmised that these results could

be due to desorption of Pb adatoms upon ligand stripping, as others have reported on the lability of excess surface Pb atoms under certain conditions.[18] Indeed, inductively coupled plasma atomic emission spectroscopy (ICP-AES) revealed that PbSe-OA nanocrystals stripped with $Et_3OBF_4$ have a nearly equimolar ratio of Pb:Se (0.97:1.00), while the initial sample had the expected lead-rich ratio of 1.22:1.00.

To explore the homogeneity in ligand stripping using this technique, we investigated the composition across the initial and treated PbSe films by nano-IR.[19] AFM images on the micrometer scale were obtained on approximately 200 nm-thick films assembled layer-by-layer on ZnSe prisms (Figure 3). Infrared spectra of the initial and stripped films
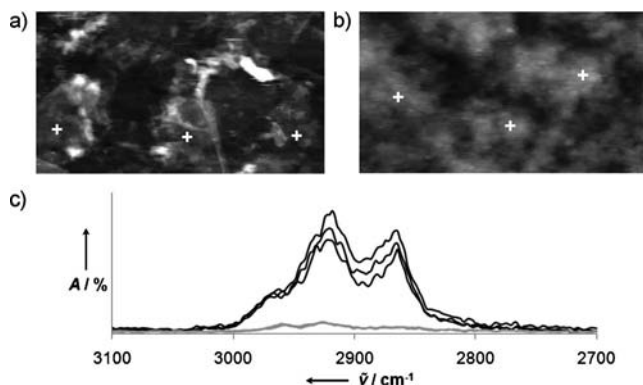


***Figure 3.*** AFM images of approximately 200 nm-thick films of a) nanocrystalline PbSe-OA and b) nanocrystalline PbSe-OA treated with $Et_3OBF_4$ in MeCN. Images are 8×14 μm and 4×8 μm in size, respectively. c) Nano-IR analysis of PbSe-OA (black) and treated (gray) films obtained at various points on each film (white crosses) showing uniform composition.

were obtained at random points across the films by irradiation through the prism and analysis of the wavelength-dependent thermal expansion pulse measured by the AFM cantilever tip. The initial PbSe-OA film showed the expected CH absorptions around 2900 cm$^{-1}$. Upon oleate stripping with $Et_3OBF_4$, significantly reduced absorption was observed uniformly across the treated film. The ability to remove insulating ligands quickly and homogeneously with no subsequent annealing should present robust, new paths for fabricating large-area thin-film devices by relatively simple and fast solution processing.

We next determined whether Meerwein's treatment had caused significant change to the size or structure of PbSe nanocrystals. To elucidate any changes in crystallinity, XRD patterns were collected for the PbSe films. As shown in Figure 4a, diffraction patterns for both initial and ligand-stripped PbSe particles were consistent with a rock-salt structure. The Scherrer formula was then used to calculate crystallite size (Table 1). The initial coherent domain size, calculated to be 10.1 nm, was similar after ligand stripping (9.5–7.9 nm). Considering the many factors contributing to broadening of diffraction peaks, the corresponding absorption spectra were also obtained (Figure 4b and c). Calculation of PbSe diameter from the first exciton peak[20] (Table 1) revealed less than 0.1 nm difference in size after stripping,
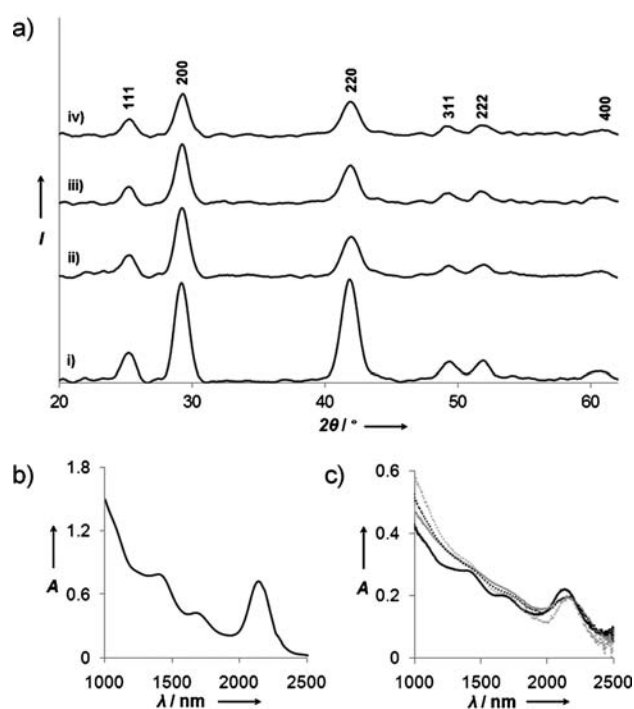


***Figure 4.*** a) XRD patterns of PbSe-OA nanocrystals before and after ligand stripping. i) PbSe-OA and PbSe-OA treated with $Et_3OBF_4$ in ii) MeCN, iii) DMF/MeCN, and iv) HMPA/MeCN. Peaks were assigned according to JCPDS file 01-078-1903. b) Absorbance of PbSe-OA in tetrachloroethylene solution. c) Diffuse reflectance of thin films: PbSe-OA (black) and PbSe after treatment with $Et_3OBF_4$ in MeCN (gray), DMF/MeCN (black dots), and HMPA/MeCN (gray dots).

***Table 1:*** Summary of particle size[a] and electrical measurements[b] for PbSe-OA and $Et_3OBF_4$-treated PbSe films.[c]

| Film | Size [nm] | $\sigma$ [S cm$^{-1}$] | Carrier concentration [cm$^{-3}$] | Mobility [cm$^2$V$^{-1}$s$^{-1}$] |
|---|---|---|---|---|
| PbSe-OA | 7.0 (10.1) | n.d.[d] | n.d.[d] | n.d.[d] |
| MeCN | 7.1 (9.5) | $1.5 \times 10^{-2}$ | $2.3 \times 10^{16}$ | 4.1 |
| DMF/MeCN | 7.1 (7.9) | $5.8 \times 10^{-2}$ | $1.4 \times 10^{18}$ | 2.6 |
| HMPA/MeCN | 7.1 (8.3) | $2.7 \times 10^{-2}$ | $6.9 \times 10^{17}$ | 2.5 |

[a] Calculated from absorbance spectra with those extracted from XRD data by using the Scherrer formula in parentheses. [b] Determined by Hall-effect measurements. [c] Two rounds of film deposition and ligand stripping were performed on glass substrates; see Supporting Information for further details. [d] Value was below instrument threshold. n.d. = not determined.

that is, neither fusing nor etching of oleate-stripped particles had occurred, aside from the noted loss of excess surface Pb adatoms evident by ICP-AES analysis.

Due to the efficient removal of insulating oleate ligands, we anticipated favorable effects on the electronic properties of the treated films. As expected, the initial PbSe-OA films were not conductive, even after extensive washing with MeCN. Conversely, oleate-stripped PbSe films were found to exhibit p-type conductivity, with $\sigma = (1.5–5.8) \times 10^{-2}$ S cm$^{-1}$ (Table 1) when measured in air. These values are comparable

to those of PbSe-OA films treated with amines on exposure to air ($\sigma = 1 \times 10^{-3}$ to $5 \times 10^{-1}$ S cm$^{-1}$), which resulted in highly conductive p-type films due to evaporation of absorbed amine molecules and subsequent doping by oxygen, hydroxyl, and water.[3a, 21] This demonstrates the ability to rapidly increase transport in films of chalcogenide nanocrystals without annealing, sintering, etching, or the use of hazardous chemical treatments, such as anhydrous hydrazine, which is an enabling technique in thin-film solution processing.

Dispersions of stripped nanocrystals, which are useful for numerous applications from nanoinks for device fabrication to biomolecular passivation, could also be obtained by using trialkyl oxonium salts (Figure 5). Typically, a dispersion of



***Figure 5.*** Dispersions of BF$_4^-$/DMF passivated nanocrystals. From left to right: ITO, AZO, TiO$_2$, α-Fe$_2$O$_3$, CdSe/ZnS ($\lambda_{em}$ = 545 nm), CdSe/ZnS ($\lambda_{em}$ = 605 nm), CdSe/CdS quantum dot/quantum rods ($\lambda_{em}$ = 619 nm), upconverting NaYF$_4$:Yb/Tm, and Ag nanocrystals.

nanocrystals in hexanes (1–20 mg mL$^{-1}$) was added to trimethyloxonium tetrafluoroborate (Me$_3$OBF$_4$) dissolved in MeCN (1–100 mM) to form a biphasic solution. After vortexing for a few seconds, the bare nanocrystals precipitated and could be isolated after addition of chloroform followed by pelleting them under centrifugation. The pellet was washed with additional portions of chloroform to remove excess Me$_3$OBF$_4$ and methyl oleate before redispersing the solid residue in DMF. This procedure substantially avoids contamination of the nanocrystal dispersion by the exogenous stripping agent, which is generally not afforded by other strategies whereby direct transfer to coordinating solvents (e.g., DMF) is implemented. A broad spectrum of nanocrystals including TiO$_2$, α-Fe$_2$O$_3$, tin-doped indium oxide (ITO), aluminum-doped zinc oxide (AZO), CdSe/ZnS core/shell quantum dots, CdSe/CdS quantum dot/quantum rods, upconverting NaYF$_4$:Yb/Tm, Ag, and FePt nanocrystals passivated by either oleate, phosphonate, or amine ligands were successfully stripped and redispersed in DMF. The resulting dispersions were stable for months at concentrations in excess of about 50 mg mL$^{-1}$. Stripping of nanocrystal dispersions by using trialkyl oxonium salts with PF$_6^-$ as counterion yielded similar results, while using SbCl$_6^-$ was less successful, attributed to the ability of this anion to function as an oxidant,[11] which again points to the sensitivity of some classes of nanocrystals to oxidizing conditions.

As with the reactions performed on thin films, it was important to determine whether the solution-phase approach was complete in its stripping of native surface ligands and that it avoided irreversible particle fusing and etching. The TEM images of the initial and treated nanocrystals (Supporting Information, Figures S6–S8) showed that their quality was retained after stripping. In general, no aggregation was observed by dynamic light scattering (DLS) of stripped nanocrystal dispersions in DMF. For example, oleylamine-passivated ITO nanocrystals with initial hydrodynamic size of 18 nm in hexanes exhibited a hydrodynamic size of 14 nm after treatment with Me$_3$OBF$_4$ (Supporting Information, Figure S9), consistent with loss of ligands with long carbon chains. Additionally, representative absorbance spectra confirmed no etching had occurred (Supporting Information, Figure S10). Unlike the PbSe nanocrystal films, dispersions of stripped nanocrystals were found by FTIR to contain adsorbed BF$_4^-$ and DMF (Supporting Information, Figure S11-S14), consistent with similar dispersions produced by using NOBF$_4$. What distinguishes the Meerwein's approach from NOBF$_4$, however, is that, for the first time, one can produce metal chalcogenide nanocrystal dispersions, which demonstrates the mildness of the procedure. For example, two different samples of CdSe/ZnS core/shell nanocrystals stripped of phosphonate ligands and re-passivated with oleate had nearly identical photoluminescence, which is exceptionally sensitive to size (i.e., no etching occurred), retention of cationic surface adatoms, and the extent of passivation of surface traps (Supporting Information, Figure S15). Films of nanocrystals passivated by BF$_4^-$ and DMF exhibited decreased interparticle spacing relative to their oleate-passivated counterparts (Supporting Information, Figure S16–S17), which should provide excellent opportunities in nanoink applications, where large-area nanocrystal-based active layers are required.

In summary, Meerwein's and related trialkyl oxonium salts have been presented as a universal class of reagents for ligand stripping of carboxylate-, phosphonate-, and amine-passivated nanocrystals. Most significantly, quantitative ligand removal was readily obtained for several important semiconductor types, including PbSe, doped ZnO, and CdSe-based heterostructures. In the atypical case of PbSe, no evidence of surface passivation by either BF$_4^-$ or solvent molecules was detected by FTIR and EDS, while supporting ICP-AES data indicated that desorption of Pb$^{II}$ adatoms accompanies ligand removal. This result may explain why PbSe nanocrystals have been particularly difficult to keep dispersed once their native ligands have been removed by this or other methods. Nevertheless, rapid yet mild ligand stripping by Meerwein's salt resulted in highly conductive PbSe films with hole mobilities as high as 4 cm$^2$ V$^{-1}$ s$^{-1}$ without the need for additional treatments. All other nanocrystal compositions surveyed showed evidence for weak adsorption of anion and solvent species, consistent with the retention of surface adatoms. These surface-adsorbed species facilitated stable colloidal dispersions in polar solvents and were amenable to subsequent ligand modification. Collectively, these qualities make Meerwein's and other trialkyl oxonium salts highly versatile chemical agents for control of nano-

crystal solubility and surface properties, which should lead to improved manipulation of nanocrystal surface composition for desired applications.

## Experimental Section

PbSe nanocrystals with average size ($7.2 \pm 0.6$ nm) and first absorption feature at 2137 nm were synthesized according to a slight modification of literature methods.[22] See Supporting Information for detailed experimental procedures.

PbSe ligand-stripping reactions were performed in a nitrogen dry box. Approximately 90–200 nm-thick nanocrystal films grown at an air/acetonitrile interface were first deposited on Si substrates. The PbSe films were then soaked in MeCN solutions of $Et_3OBF_4$ (50–100 mM) or $NOBF_4$ (50 mM) for 5 min. Ligand stripping in the presence of cosolvents was carried out with 1M DMF or HMPA in MeCN. All treated films were gently washed five times with 800 µL portions of MeCN followed by hexanes. The initial PbSe-OA films were routinely washed ten times with 800 µL portions of MeCN to ensure accurate comparisons with treated films, as oleate ligands can be removed by excessive washing under some conditions.[23] Analogous samples were prepared under identical conditions on clean glass substrates for XRD, diffuse-reflectance measurements, and conductivity measurements. For conductivity measurements, two rounds of film deposition and treatment were performed on clean glass substrates to give approximately 200 nm-thick films largely devoid of through-film cracks.

SEM images were recorded on a Zeiss Gemini Ultra-55 Analytical scanning electron microscope with a beam energy of 5 kV and an In-Lens detector. An inbuilt EDS detector was used for elemental analysis. XRD was performed on a Bruker Gadds-8 diffractometer with a $Cu_{K\alpha}$ source operating at 40 kV and 20 mA. FTIR spectra were obtained on a PerkinElmer Spectrum One FTIR Spectrometer on AgCl or double-side-polished Si substrates or on a ZnSe prism by using an HATR sampling accessory. Atomic emission spectroscopy was performed on a Varian 720-ES ICP optical emission spectrometer by using an argon plasma. Nano-IR measurements were obtained at Anasys Instruments, Santa Barbara, CA, on an Anasys Instruments NanoIR platform. Absorbance spectra were recorded on a Varian Cary 5000 UV/Vis/NIR spectrophotometer. Diffuse-reflectance spectra were determined on an ASD Inc. Quality Spec Pro UV/Vis spectrometer with MugLite attachment and Spectralon reference. Hall-effect measurements were obtained in air by using an Ecopia HMS-5000 Hall effect measurement system. Film thicknesses were determined on a Veeco Dektak 150 Surface Profilometer. Dynamic light scattering (DLS) data were obtained with a Malvern Zetasizer Nano ZS instrument.

[1] a) Y. W. Jun, J. S. Choi, J. Cheon, *Angew. Chem.* **2006**, *118*, 3492–3517; *Angew. Chem. Int. Ed.* **2006**, *45*, 3414–3439; b) J. Park, J. Joo, S. G. Kwon, Y. Jang, T. Hyeon, *Angew. Chem.* **2007**, *119*, 4714–4745; *Angew. Chem. Int. Ed.* **2007**, *46*, 4630–4660.

[2] a) J. Aldana, Y. A. Wang, X. Peng, *J. Am. Chem. Soc.* **2001**, *123*, 8844–8850; b) T. Hanrath, D. Veldman, J. J. Choi, C. G. Christova, M. M. Wienk, R. A. J. Janssen, *ACS Appl. Mater. Interfaces* **2009**, *1*, 244–250.

[3] a) M. Law, J. M. Luther, Q. Song, B. K. Hughes, C. L. Perkins, A. J. Nozik, *J. Am. Chem. Soc.* **2008**, *130*, 5974–5985; b) J. E. B.

Katari, V. L. Colvin, A. P. Alivisatos, *J. Phys. Chem.* **1994**, *98*, 4109–4117; c) M. Kuno, J. K. Lee, B. O. Dabbousi, F. V. Mikulec, M. G. Bawendi, *J. Chem. Phys.* **1997**, *106*, 9869–9882.

[4] a) M. Drndić, M. V. Jarosz, N. Y. Morgan, M. A. Kastner, M. G. Bawendi, *J. Appl. Phys.* **2002**, *92*, 7498–7503; b) A. W. Wills, M. S. Kang, A. Khare, W. L. Gladfelter, D. J. Norris, *ACS Nano* **2010**, *4*, 4523–4530; c) S. V. Voitekhovich, D. V. Talapin, C. Klinke, A. Kornowski, H. Weller, *Chem. Mater.* **2008**, *20*, 4545–4547; d) B. A. Ridley, B. Nivi, J. M. Jacobson, *Science* **1999**, *286*, 746–749; e) S. J. Baik, K. Kim, K. S. Lim, S. Jung, Y. C. Park, D. G. Han, S. Lim, S. Yoo, S. Jeong, *J. Phys. Chem. C* **2011**, *115*, 607–612.

[5] a) K. S. Leschkies, T. J. Beatty, M. S. Kang, D. J. Norris, E. S. Aydil, *ACS Nano* **2009**, *3*, 3638–3648; b) J. M. Luther, M. Law, Q. Song, C. L. Perkins, M. C. Beard, A. J. Nozik, *ACS Nano* **2008**, *2*, 271–280; c) Y. Liu, M. Gibbs, J. Puthussery, S. Gaik, R. Ihly, H. W. Hillhouse, M. Law, *Nano Lett.* **2010**, *10*, 1960–1969; d) M. V. Kovalenko, D. V. Talapin, M. A. Loi, F. Cordella, G. Hesser, M. I. Bodnarchuk, W. Heiss, *Angew. Chem.* **2008**, *120*, 3071–3075; *Angew. Chem. Int. Ed.* **2008**, *47*, 3029–3033; e) D. V. Talapin, C. B. Murray, *Science* **2005**, *310*, 86–89.

[6] a) R. Tangirala, J. L. Baker, A. P. Alivisatos, D. J. Milliron, *Angew. Chem.* **2010**, *122*, 2940–2944; *Angew. Chem. Int. Ed.* **2010**, *49*, 2878–2882; b) A. Llordes, A. T. Hammack, R. Buonsanti, R. Tangirala, S. Aloni, B. A. Helms, D. J. Milliron, *J. Mater. Chem.* **2011**, *21*, 11631–11638; c) M. V. Kovalenko, M. Scheele, D. V. Talapin, *Science* **2009**, *324*, 1417–1420; d) M. V. Kovalenko, M. I. Bodnarchuk, J. Zaumseil, J. S. Lee, D. V. Talapin, *J. Am. Chem. Soc.* **2010**, *132*, 10085–10092; e) M. V. Kovalenko, B. Spokoyny, J. S. Lee, M. Scheele, A. Weber, S. Perera, D. Landry, D. V. Talapin, *J. Am. Chem. Soc.* **2010**, *132*, 6686–6695.

[7] a) X. Michalet, F. F. Pinaud, L. A. Bentolila, J. M. Tsay, S. Doose, J. J. Li, G. Sundaresan, A. M. Wu, S. S. Gambhir, S. Weiss, *Science* **2005**, *307*, 538–544; b) T. Zhang, J. Ge, Y. Hu, Y. Yin, *Nano Lett.* **2007**, *7*, 3203–3207; c) W. W. Yu, E. Chang, C. M. Sayes, R. Drezek, V. L. Colvin, *Nanotechnology* **2006**, *17*, 4483–4487; d) M. Liong, H. Shao, J. B. Haun, H. Lee, R. Weissleder, *Adv. Mater.* **2010**, *22*, 5168–5172; e) N. Bogdan, F. Vetrone, G. A. Ozin, J. A. Capobianco, *Nano Lett.* **2011**, *11*, 835–840.

[8] a) H. Meerwein, G. Hinz, P. Hofmann, E. Kroning, E. Pfeil, *J. Prakt. Chem.* **1937**, *147*, 257–285; b) H. Meerwein, E. Battenberg, H. Gold, E. Pfeil, G. Willfang, *J. Prakt. Chem.* **1939**, *154*, 83–156; c) H. Meerwein, *Organic Syntheses Coll. Vol. 5* **1973**, *5*, 1080; H. Meerwein, *Org. Synth.* **1966**, *46*, 113.

[9] A. Dong, X. Ye, J. Chen, Y. Kang, T. Gordon, J. M. Kikkawa, C. B. Murray, *J. Am. Chem. Soc.* **2011**, *133*, 998–1006.

[10] Addition of $NOBF_4$ to both aluminum-doped ZnO and ZnO nanocrystals resulted in decomposition.

[11] N. G. Connelly, W. E. Geiger, *Chem. Rev.* **1996**, *96*, 877–910.

[12] A. Nag, M. V. Kovalenko, J. S. Lee, W. Liu, B. Spokoyny, D. V. Talapin, *J. Am. Chem. Soc.* **2011**, *133*, 10612–10620.

[13] a) M. A. Caldwell, A. E. Albers, S. C. Levy, T. E. Pick, B. E. Cohen, B. A. Helms, D. J. Milliron, *Chem. Commun.* **2011**, *47*, 556–558; b) J. S. Owen, J. Park, P. E. Trudeau, A. P. Alivisatos, *J. Am. Chem. Soc.* **2008**, *130*, 12279–12281.

[14] a) F. W. Wise, *Acc. Chem. Res.* **2000**, *33*, 773–780; b) I. Kang, F. W. Wise, *J. Opt. Soc. Am. B* **1997**, *14*, 1632–1646; c) J. M. An, A. Franceschetti, S. V. Dudiy, A. Zunger, *Nano Lett.* **2006**, *6*, 2728–2735.

[15] R. K. Haynes, C. Indorato, *Aust. J. Chem.* **1984**, *37*, 1183–1194.

[16] See Figure S1 of the Supporting Information for related TEM images.

[17] Films stripped in HMPA also showed no stretching bands attributable to $BF_4^-$ or solvent (see Supporting Information, Figure S4).

[18] a) Q. Dai, Y. Zhang, Y. Wang, Y. Wang, B. Zou, W. W. Yu, M. Z. Hu, *J. Phys. Chem. C* **2010**, *114*, 16160–16167; b) Z. Lingley, S. Lu, A. Madhukar, *Nano Lett.* **2011**, *11*, 2887–2891.

[19] a) K. Kjoller, J. R. Felts, D. Cook, C. B. Prater, W. P. King, *Nanotechnology* **2010**, *21*, 185705; b) A. Dazzi, F. Glotin, R. Carminati, *J. Appl. Phys.* **2010**, *107*, 124519; c) R. P. Dazzi, F. Glotin, J. M. Ortega, *Infrared Phys. Technol.* **2006**, *49*, 113–121.

[20] Q. Dai, Y. Wang, X. Li, Y. Zhang, D. J. Pellegrino, M. Zhao, B. Zou, J. Seo, Y. Wang, W. W. Yu, *ACS Nano* **2009**, *3*, 1518–1524.

[21] See Figure S5 for XPS spectra of initial and treated films.

[22] a) W. W. Yu, J. C. Falkner, B. S. Shih, V. L. Colvin, *Chem. Mater.* **2004**, *16*, 3318–3322; b) J. Joo, J. M. Pietryga, J. A. McGuire, S. H. Jeon, D. J. Williams, H. L. Wang, V. I. Klimov, *J. Am. Chem. Soc.* **2009**, *131*, 10620–10628.

[23] I. L. Bolotin, D. J. Asunskis, A. M. Jawaid, Y. Liu, P. T. Snee, L. Hanley, *J. Phys. Chem. C* **2010**, *114*, 16257–16262.